The making of Andersen's liquefaction chart

Sabaliauskas, Tomas; Ibsen, Lars Bo

Publication date:
2017

Document Version
Publisher's PDF, also known as Version of record

DEPARTMENT OF CIVIL ENGINEERING
AALBORG UNIVERSITY

The Making of Andersen's liquefaction chart

Tomas Sabaliauskas
Lars Bo Ibsen

ISSN 1901-7278
DCE Technical Memorandum No. 62

Aalborg University
Department of Civil Engineering
Group Name

DCE Technical Memorandum No. 62

The Making of Andersen's liquefaction chart

by

Tomas Sabaliauskas
Lars Bo Ibsen

2017

Scientific Publications at the Department of Civil Engineering

Technical Reports are published for timely dissemination of research results and scientific work carried out at the Department of Civil Engineering (DCE) at Aalborg University. This medium allows publication of more detailed explanations and results than typically allowed in scientific journals.

Technical Memoranda are produced to enable the preliminary dissemination of scientific work by the personnel of the DCE where such release is deemed to be appropriate. Documents of this kind may be incomplete or temporary versions of papers—or part of continuing work. This should be kept in mind when references are given to publications of this kind.

Contract Reports are produced to report scientific work carried out under contract. Publications of this kind contain confidential matter and are reserved for the sponsors and the DCE. Therefore, Contract Reports are generally not available for public circulation.

Lecture Notes contain material produced by the lecturers at the DCE for educational purposes. This may be scientific notes, lecture books, example problems or manuals for laboratory work, or computer programs developed at the DCE.

Theses are monograms or collections of papers published to report the scientific work carried out at the DCE to obtain a degree as either PhD or Doctor of Technology. The thesis is publicly available after the defence of the degree.

Latest News is published to enable rapid communication of information about scientific work carried out at the DCE. This includes the status of research projects, developments in the laboratories, information about collaborative work and recent research results.

Published 2017 by
Aalborg University
Department of Civil Engineering
Thomas Manns vej 23, 9220
Aalborg, Denmark

Printed in Aalborg at Aalborg University

ISSN 1901-7278
DCE Technical Memorandum No. 62

The making of Andersen's liquefaction chart

Tomas Sabaliauskas, Lars Bo Ibsen.

1. ABSTRACT

This technical report contains supplementary material describing procedures used in triaxial testing result analysis. The content explains concepts relevant to very specific case study where triaxial test results were analyzed.

Andersen's chart (Andersen & Berre, 1999) is a graphical method of observing cyclic soil response. It allows to separate cyclic stable soil states from cyclic unstable. Normally, the chart is obtained by manually fitting experimental measurements into a data plot. Here, steps of automating the procedure and normalizing the chart are provided.

2. INTRODUCTION

Cyclic undrained sand response is used in offshore engineering, to predict soil to structure interaction. Knut H. Andersen introduced a chart which describes undrained cohesionless soil response (Andersen & Berre, 1999). His chart was generated using dynamic, single diameter height, frictionless triaxial apparatus at Aalborg University by Troya, A. & Sabaliauskas, T., (2014). Andersen's method was modified during tests at AAU, improved methods of normalizing the chart, and algorithms which generate the chart atomically, were introduced. This makes generating the chart – more efficient, and after the chart is generated – improved normalizing allows to use it in a wider scope of application.

To obtain the Andersen's chart, undrained cyclic tests were done with varying stress amplitude $\boldsymbol{\tau_{cy}}$ and average stress values $\boldsymbol{\tau_a}$ (illustration of soil behavior during cyclic loading is given in Fig.1). If some particular configuration of amplitude and mean value leads to instability within soil – the Andersen's chart will predict it. Before each test $\boldsymbol{\tau_{cy}}$ and $\boldsymbol{\tau_a}$ were selected to target a specific position on Andersen's chart – thus higher concentration of measurements could be clustered in critical regions of the chart. As more data points were collected, position of the "failure" limit became more evident – and measurements clustered around the failure line. Automated algorithms, used to generate parts of the chart from incomplete data, allowed to target the failure line more efficiently.

3. SOIL USED

Silty sand taken from a wind turbine farm in Frederichaven, Denmark is used for testing. All samples are tested from initial conditions of pore pressure $\Delta Up = 200$[kPa], initial confining pressure $p'_0=60$[kPa], anisotropic K0 consolidation is chosen as the initial state reassembling in situ soil state for cohesionless soil with friction angle of approximately $\varphi=39°$ giving initial sample state of $\sigma_1=161$[kPa] $\sigma_3=60$[kPa]; Samples are dry tamped to 80% relative density (maximum porosity $e_{max}=1.05$; minimum porosity $e_{min}=0.64$)

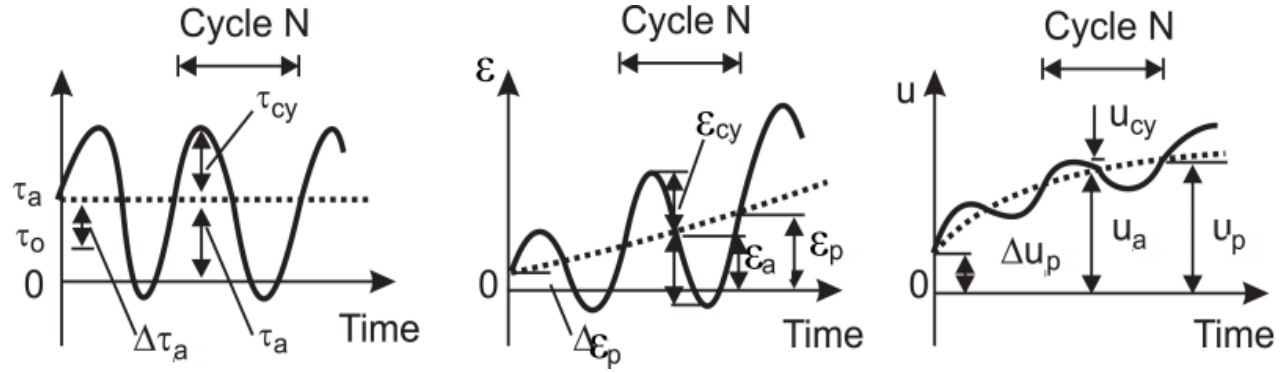

Eq. 1

Fig. 1 cyclic, average and plastic components of shear stress, strain and pore pressure (Andersen & Berre, 1999)

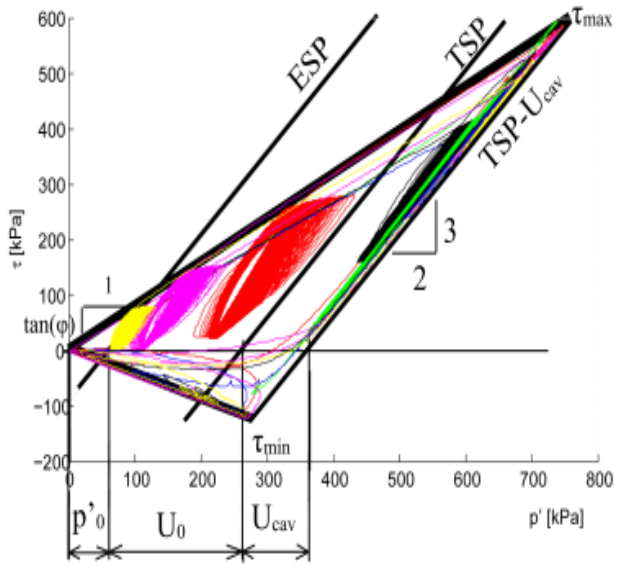

Fig. 2 Multiple cyclic tests followed by ultimate bearing capacity crushing. Contained in a "triangle" consisting of friction angles and cavitation limit.

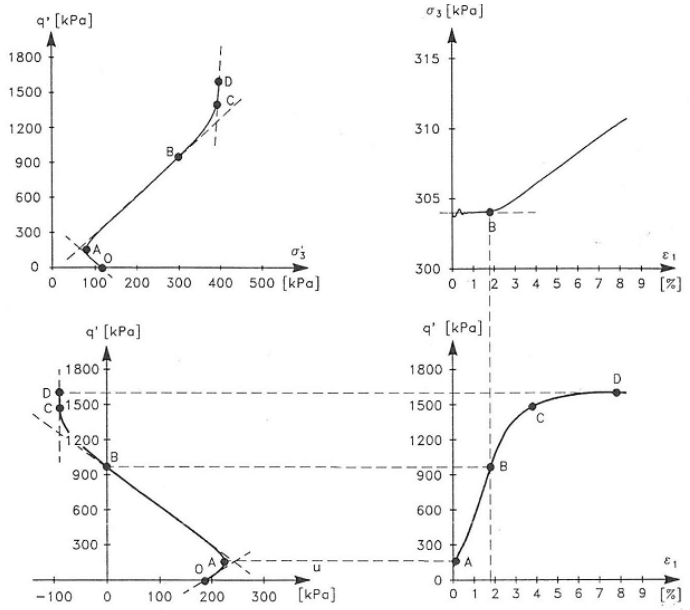

Fig. 3 pore pressure and strain of Monotonic CU triaxial on AAU sand 1. (Ibsen, 1995)

4. UNDRAINED BEARING CAPACITY (NORMALIZING)

If the sample was loaded drained it would follow the Effective Stress Path (ESP line in Fig. 2). Undrained dilative sand deaviates from the ESP path, and develops up the hidrostatic effective stress axis, until pore water reaches near -100kPa. Thus, both drained and undrained sand cross the same effective stress envelope, but they cross it in different positions – despite identical initial state.

When dense sand is compressed to failure undrained, it dilates along some friction angle (points A-C in Fig. 3). Dilation will force the confining pressure p' to rise (while pore pressure is dropping). At some point pore pressure will reach near -100[kPa] and turn into gas (cavitate, at room temperature). As the stiffness of pore water is lost, water evaporates, specimen transitions into drained response - and the failure envelope is reached. Yielding is triggered (C-D in Fig. 3, TSP-Ucav in Fig. 2).

Cavitation plays a definitive role in response of undrained, dense, cohesionless soil. It provides a strict limit which ultimate strength adheres to (Fig. 2, Fig. 5) (Ibsen, 1994) (Ibsen, 1995)(Nielsen & Ibsen, 2013) (Troya & Sabaliauskas, 2014).. This was not taken into account in original work by Andersen (Fig. 4). But since the maximum and minimum bearing capacity can be found from equations (2-3), the Andersens chart can be normalized within these limits.

$$p'_{LOCK} = p'_0 + U_0 - Ucav \qquad (1)$$

$$\tau_{\max} = -p'_{LOCK} \cdot \sin(\varphi)/(\sin(\varphi) - 1) \qquad (2)$$

$$\tau_{\min} = -p'_{LOCK} \cdot \sin(\varphi)/(\sin(\varphi) + 1) \qquad (3)$$

The provided bearing capacity expressions were suggested as a potential choice for normalising the Andersen's chart by Nielsen & Ibsen, (2013).

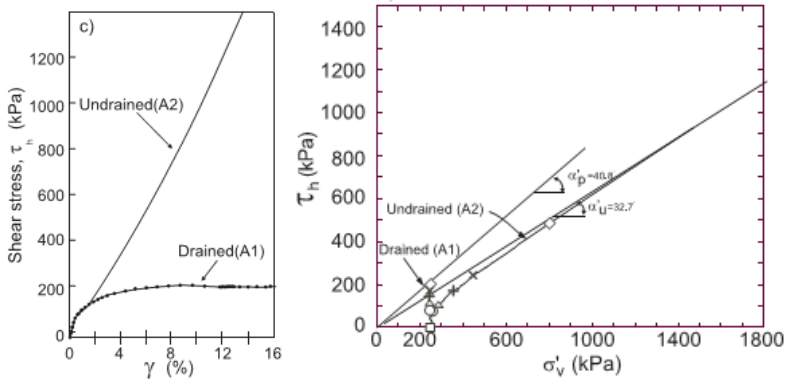

Fig. 4 Andersen's stress-strain chart and principal stress DSS test – undrained response does not reach plastic failure due to extremely high initial pore pressure available for dilation. (Andersen & Berre, 1999)

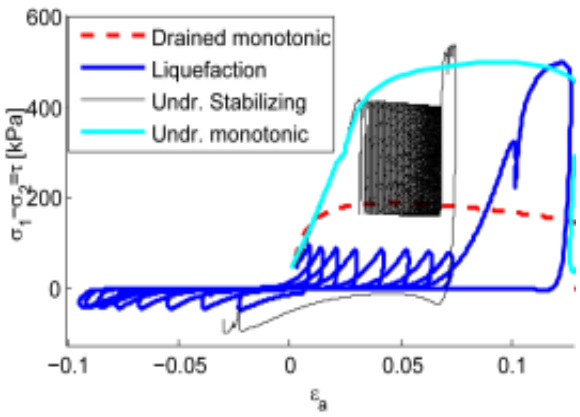

Fig. 5 Undrained strength testing in various testing cases.

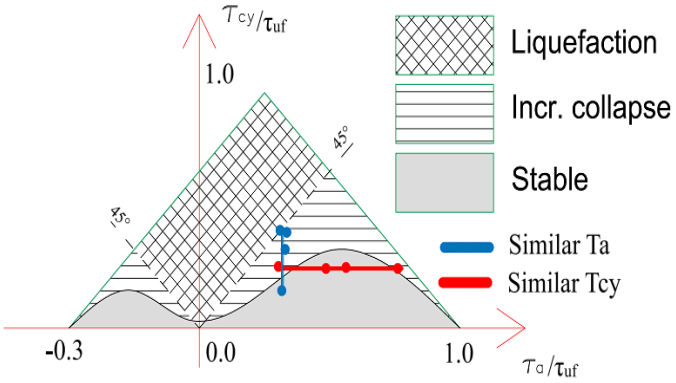

Fig. 6 Normalized schematic of observed response

5. THE ANDERSENS CHART

Each sample starts from anisotropic – K0 state which is loaded over 1 hour of slow, drained loading. Then the valves are closed and a cyclic, sinusoidal shaped load is applied. No additional preloading was applied.

Tests revealed 3 distinct zones within the Andersen's chart.

1. Liquefaction failure (two way loaded)
2. Incremental failure (one way loaded case 1)
3. Stabilization (One way loaded case 2)

Stress reversal causes liquefaction, and incremental collapse was encountered if one way loaded cycles were not too far from being two-way loaded. (Fig. 6). (Ibsen, 1994) (Ibsen, 1995) (Andersen & Berre, 1999) (Nielsen & Ibsen, 2013) (Sabaliauskas & Troya, 2014)

Testing was optimized toward finding an isoparametric line which shows stress states reaching 10% axial strain at 1000th cycle. 1000 cycle limit was chosen because it approximates the number of waves during a 3 hour storm peak in typical storm in North Sea. During testing it was found that 1000 cycles produce a very steep function separating stable response from unstable, thus clustering around this line was essential. To illustrate the need for "targeting the line", a line with similar Tcy is shown in In fig Fig.6. Notice, how holding Tcy constant crosses the "failure line" twice. The objective of testing was to find settings as close to the "failure line" as plausible, by modifying $\boldsymbol{\tau_a}$, while Tcy is held constant. Alternatively, if Ta is held constant – $\boldsymbol{\tau_{cy}}$ position can be modified.

Notice, both $\boldsymbol{\tau_a}$ and $\boldsymbol{\tau_{cy}}$ are absolute stresses (not effective stress). The original chart, proposed by Andersen, was normalized using drained stress σ'_{vc} (Fig.8). Normalizing undrained response with drained strength is not the correct approach. Undrained ultimate strength for dense, cohesionless soil can be reliably quantified as shown previously, by formulae 2 and 3. When using the undrained yield strength to normalize undrained Andersen's chart – the axis become contained between -0.3 and 1, as visible in Fig.6 (note, the value on the negative side is not fixed to -0.3, the value depends on the friction angle).

6. TRIANGULATING THE ANDERSEN'S CHART

While linear interpolation with constant Tcy or constant Ta is a valid option, it is not a very efficient way of generating a surface plot. A better approach would be to plot what is "visible" at each step, using measurements available before the final version of the chart is known. Then, parts of the picture, which need "improved definition", could be targeted. This was accomplished by meshing the test data with triangular surfaces, and then color plotting the 3d surfaces along the Z axis. With each test the triangulated surface would update itself automatically, and the researcher could choose which part will be refined further during the next test.

Each data point has 3 coordinates - $\boldsymbol{\tau_a}$, $\boldsymbol{\tau_{cy}}$ and the number of cycles **n**. The value of **n** depends on "failure strain limit" defined by the user (as illustrated in Fig.7). And number of cycles leading to each strain increment is obtained using two sided peak detection (shown in Fig.8).

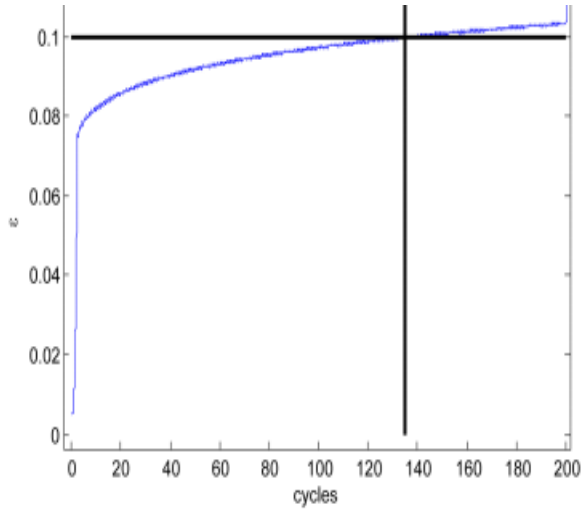

Fig. 7 Strain development with cycles and Strain peak detection.

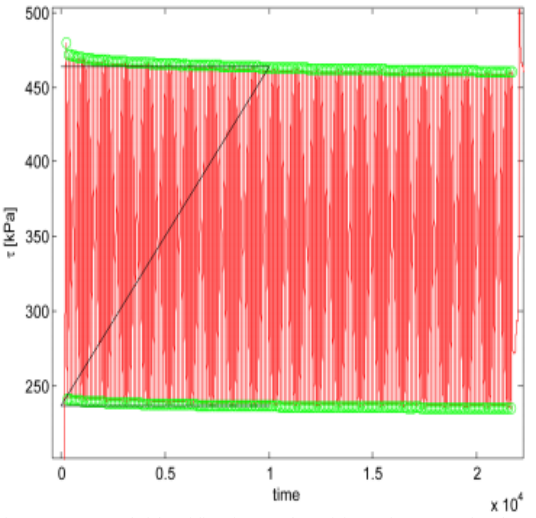

Fig. 8 stress peak identification and position of averaged values

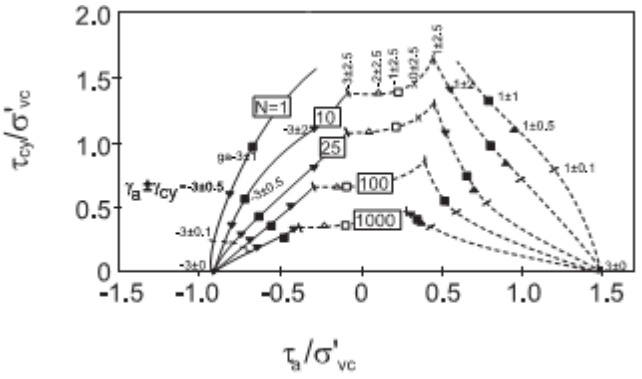

Fig. 9 Original Andersen's chart for undrained soil response (normalized by drained confining pressure)

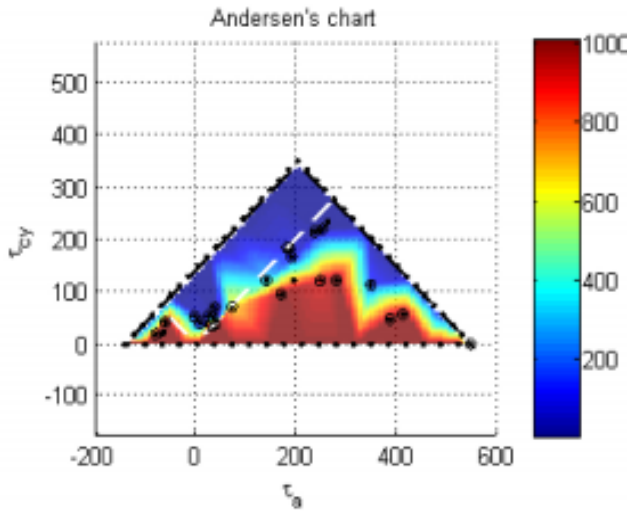

Fig. 10 Andersen's chart before manual corrections. Dots indicate tested points. Fully autonomous generated by algorithm – some triangulation error present.

Collection of 3 coordinates ($\boldsymbol{\tau_a}$, $\boldsymbol{\tau_{cy}}$ and **n**), obtained from testing is used together with collection of points set manually. If the cycle amplitude $\boldsymbol{\tau_{cy}}$=0[kPa], no cyclic loading is applied. This is equivalent to monotonic loading, which does not fail until $\boldsymbol{\tau_a}$ reaches the ultimate undrained failure. Thus, for all points where $\boldsymbol{\tau_{cy}}$=0[kPa], **n**=1000 cycles. Similarly, if ($\boldsymbol{\tau_a}$+$\boldsymbol{\tau_{cy}}$)>$\boldsymbol{\tau_{max}}$ or ($\boldsymbol{\tau_a}$-$\boldsymbol{\tau_{cy}}$)<$\boldsymbol{\tau_{min}}$ the sample will cross the ultimate strength before completing the first cycle. Thus the outer perimeter of the triangle is set to **n**=0 cycles.

At this point the chart can be interpolated by triangulation. A surface is formed by connecting the nearest points into a triangles (Delaunay triangulation). As more tests are done, definition of the chart is increased. Fig. 10 shows a chart near its final stages. However, there are some final changes that need to be done - cases where uncertainty is encountered by Delaunay triangulation algorithm. The uncertainty can be solved by either making an additional test, to provide an additional point of $\boldsymbol{\tau_a}$, $\boldsymbol{\tau_{cy}}$ and **n** coordinates. Or, the required values of $\boldsymbol{\tau_a}$, $\boldsymbol{\tau_{cy}}$ and **n** can be linearly interpolated between two measurement points to fine-tune the triangle edges.

7. FINE TUNING TRIANGLE EDGES

Given 4 points, there are 2 ways to connect them into triangles. Both are illustrated in Fig.11. If a 5th point is added by interpolating it on one of the 2 plausible lines, the user can "flip" the edge towards the preferred outcome. Thus, the final chart will have 3 sets of $\boldsymbol{\tau_a}$, $\boldsymbol{\tau_{cy}}$ and **n** coordinates:

1. Test results
2. Boundary points
3. Edge flipping interpolation

And the resulting chart is shown in Fig.12.

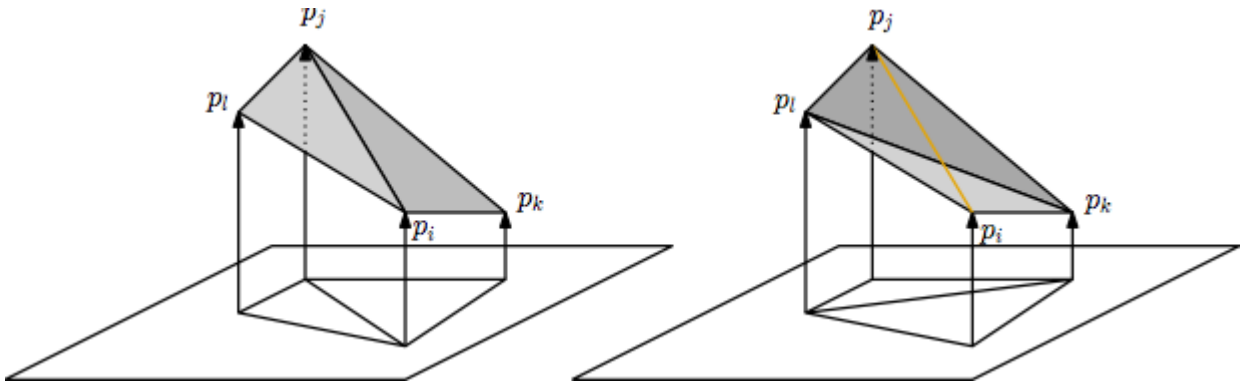

Fig. 11 "Edge flipping". There are 2 ways of connecting 4 points into triangles. Manual identification of the correct one might be necessary.

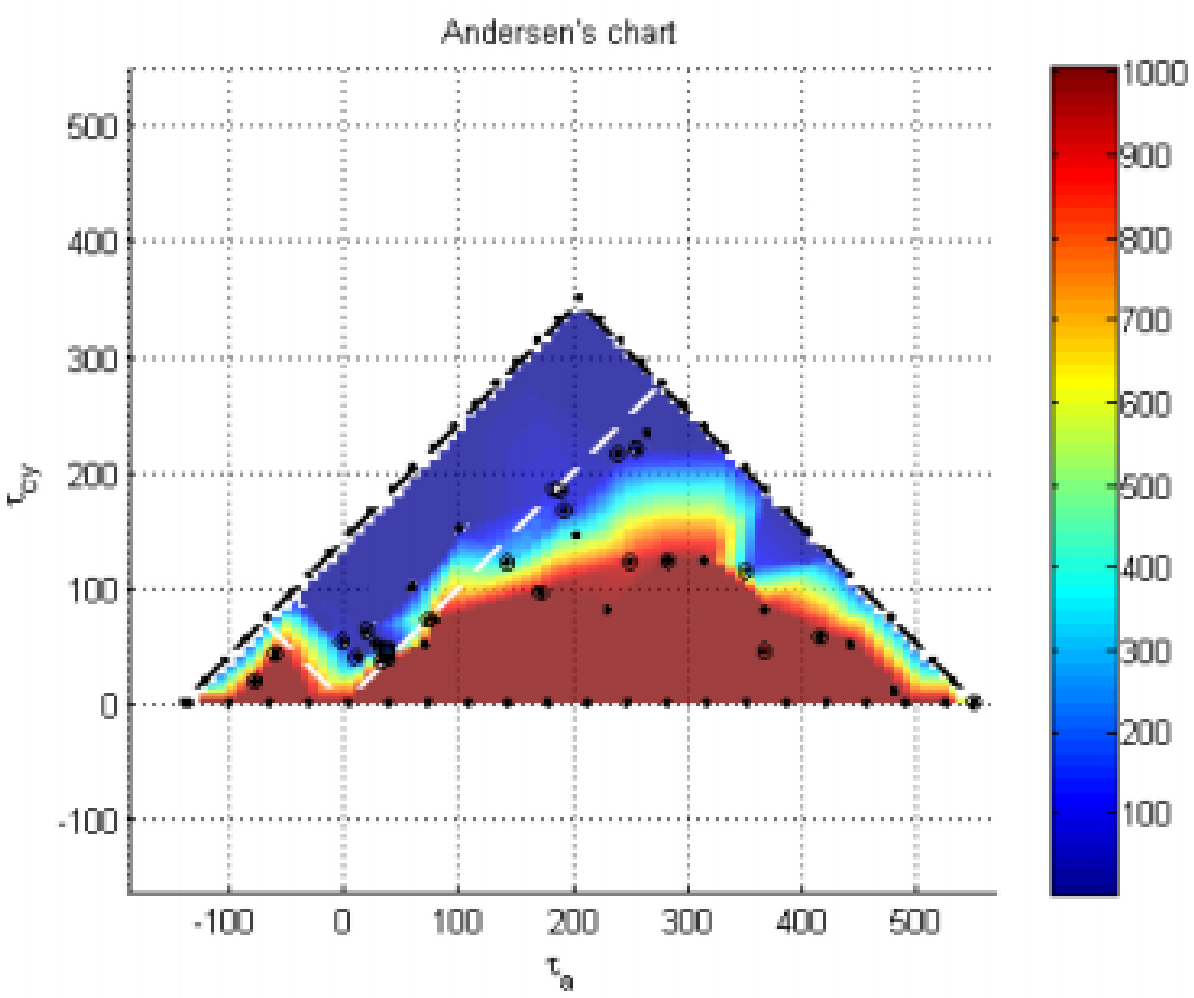

Fig. 12 Andersen's chart for Frederic haven silty sand – not normalized, raw data for 10% axial strain limit.

8. BIBLIOGRAPHY

Andersen, K. & Berre, . T., 1999. *Behaviour of a dense sand under monotonic and cyclic loading comportemen,* Amsterdam: European Conference on Soil Mechanics and Geotechnical Engineering.

Andersen, K. H., 2009. *Bearing capacity under cyclic loading — offshore,.* Oslo: The 21st Bjerrum.

Hettler, A. & Vardoulakis, I., 1984. *Behaviour of dry sand tested in a large triaxial apparatus.* s.l.:Geotechnique 34.2 (1984): 183-197..

Ibsen, L. B., 1994. *The stable state in cyclic triaxial testing on sand.* Aalborg: Soil Dynamics and Earthquake Engineering 13 (1994) 63-72 .

Ibsen, L. B., 1995. *The Static and Dynamic Strength of Sand.* Copenhagen: European Conference on Soil Mechanics and Foundation Engineering.

Nielsen, S. D. & Ibsen, L. B., 2013. s.l.:International Society of Offshore and Polar Engineers.

Praastrup, U., Jakobsen, K. P. & Ibsen, L. B., 1999. *Two Theoretically Consistent Methods for Analysing Triaxial Tests.* Aalborg: Computers and Geotechnics. Vol. 25(1999), pp. 157-170.

Sabaliauskas, T. & Troya, A., 2014. *Observations during static and cyclic undrained loading of dense Aalborg University sand no. 1.* Aalborg: DCE Technical Memorandum No. 43.

Shajarati, A., Sørensen, K. W., Dam, S. K. & Ibsen, L. B., 2012. *Manual for Cyclic Triaxial Test.* Aalborg: DCE Technical Report No. 114.

Troya, A. & Sabaliauskas, T., 2014. *Cyclic behaviour of undrained dense Aalborg University sand no. 1.* Aalborg: DCE Technical Memorandum. Department of Civil Engineering, Aalborg University,.

ISSN 1901-7278
DCE Technical Memorandum No. 62